01 Jan 2020

Measurement of Sub-2 Nm Stable Clusters during Silane Pyrolysis in a Furnace Aerosol Reactor

Miguel Vazquez-Pufleau

Yang Wang
Missouri University of Science and Technology, yangwang@mst.edu

Pratim Biswas

Elijah Thimsen

Recommended Citation

M. Vazquez-Pufleau et al., "Measurement of Sub-2 Nm Stable Clusters during Silane Pyrolysis in a Furnace Aerosol Reactor," *Journal of Chemical Physics*, vol. 152, no. 2, American Institute of Physics (AIP), Jan 2020.
The definitive version is available at https://doi.org/10.1063/1.5124996

The Journal of Chemical Physics ARTICLE scitation.org/journal/jcp

Measurement of sub-2 nm stable clusters during silane pyrolysis in a furnace aerosol reactor

Cite as: J. Chem. Phys. 152, 024304 (2020); doi: 10.1063/1.5124996
Submitted: 22 August 2019 • Accepted: 16 December 2019 •
Published Online: 9 January 2020

Miguel Vazquez-Pufleau,[1,2,a),b)] Yang Wang,[1,3,a)] Pratim Biswas,[1] and Elijah Thimsen[2]

AFFILIATIONS

[1]Aerosol and Air Quality Research Laboratory, Department of Energy, Environmental & Chemical Engineering, Washington University in St. Louis, St. Louis, Missouri 63130, USA
[2]Interface Research Group, Department of Energy, Environmental & Chemical Engineering, Washington University in St. Louis, St. Louis, Missouri 63130, USA
[3]Department of Civil, Architectural and Environmental Engineering, Missouri University of Science and Technology, Rolla, Missouri 65401, USA

[a)]**Contributions:** M. Vazquez-Pufleau and Y. Wang contributed equally to this work.
[b)]**Author to whom correspondence should be addressed:** miguel@wustl.edu

ABSTRACT

The initial stages of particle formation are important in several industrial and environmental systems; however, the phenomenon is not completely understood due to the inability to measure cluster size distributions. A high resolution differential mobility analyzer with an electrometer was used to map out the early stages of Si particle formation from pyrolysis of SiH_4 in a furnace aerosol reactor. We detected for the first time subnanometer stable clusters from silane pyrolysis, and the diameter was measured to be about 0.7 nm. This diameter is within the range of probable sizes that the reported families of critical silane clusters could have based on their actual molecular structure. The size distributions of negative clusters are also mapped out. In addition, gas chromatography mass spectrometry, and transmission electron microscopy characterizations of the clusters and primary particles are used to assess their mechanistic roles in aerosol dynamics of the initial stages of particle formation.

INTRODUCTION

Early stages of silicon nanoparticle formation by silane pyrolysis are important for numerous industrial processes including efficient and cost effective refining silicon for electronics,[1,2] photovoltaics,[3,4] batteries,[5,6] and other systems. Silicon nucleation has historically been explained using a polymerization approach, where silane reacts with itself, activated by the carrier gas, to form dimers, trimers, tetramers, and larger silicon hydrides,[7,8] polymerizing until the forward reaction is more favorable than the backward reaction at the given conditions, which ends the reversible reaction interplay and yields nucleation. Such a polymerization mechanism is supported by two observations. First, the rates of aerosol formation when the precursor is a larger polysilane chain are enhanced compared to those of monosilane.[1] Second, there is a delay of aerosol formation after the onset of silane pyrolysis.[9] Therefore, the kinetics of silane pyrolysis is highly relevant for understanding and predicting the nucleation rate of silicon nanoparticles. Several reaction kinetic models and mechanisms[10] have been proposed for the gross pyrolysis reaction of silane, $SiH_{4(g)} \rightarrow Si_{(s)} + 2H_{2(g)}$. Girshick *et al.*[11] proposed 100 intermediate species and 400 reactions, Kremer *et al.*[12] 33 reactions, Giunta *et al.*[13] 18 reactions, and Kleijn *et al.*[14] 10 reactions and five intermediate species. To incorporate the reaction kinetics into a nucleation theory of silane pyrolysis, the critical cluster size needs to be incorporated into the reaction kinetics.

There are conceptual differences in the description of critical clusters between physical and chemical nucleation systems. In physical nucleation, there is an equilibrium in the rate of monomers going from one phase to the other. The overall free energy is expected to increase as a function of size upon reaching a maximum at the critical cluster size and then decrease again. Clusters larger than this critical size are expected to be more likely to grow into larger particles than to break apart. Smaller clusters than the critical size are more likely to shrink than to grow. For a chemical nucleation process analogous to silicon hydride particle formation via silane pyrolysis, the free energy change as a function of particle size is, in contrast to physical nucleation, not necessarily a smooth function. The free energy might go through multiple local maxima each of them behaving as a bottleneck in the growth process. At the end, the free energy change depends on the amount of Si and H atoms as well as on the type of bonding and chemical structure of the clusters.[15] Based on these definitions, a cluster in physical nucleation is always in an unstable equilibrium where a minor change in the conditions might drive the cluster to change rapidly by losing or gaining more monomers. On the other hand, for chemical nucleation, a cluster might lay in a local maximum and the energy required to drive it forward or backward in the reaction pathway might require significant energy. Even more, if the cluster persists through a wide range of experimental and sampling conditions, it is called for the purposes of this manuscript as a "stable cluster." Such a stable cluster displays a persistent nature but should not be confused on its mechanisms of formation with the one expected based on classical nucleation theory (CNT) of a physical process, where a critical cluster is very unstable and might easily tip into one or the other direction and either grow or disappear rapidly. In any case, the critical cluster size is the smallest size required for a particle to have a higher likelihood to grow than to decompose.

For silane pyrolysis, the critical cluster size has been determined by *ab initio* calculations. Wong *et al.*[16] proposed that the amount of silicon atoms (n) in stable silicon hydride (Si_nH_m) clusters must be at least seven. On the other hand, studies by Girshick *et al.*,[11] Swihart *et al.*,[17] and Nijhawan *et al.*[18] suggested that n must be at least ten in order to produce a stable silicon hydride. The highest value possible of m (the amount of H atoms) in the formula might be 2n + 2 for linear and single bonded chains. The minimum value of m reported is equal to or even slightly lower than the amount of silicon atoms. To the best of our knowledge, there are no reports of experimental measurements of silicon hydride critical clusters. This was primarily due to the inability to measure such small clusters containing 7

TABLE I. Selected interesting potential mechanistic roles played by the stable cluster in new particle formation and growth. (+) indicates the observation that supports the mechanism. (—) indicates the observation that does not support the mechanism. The observation number is described in the "Numbered observation summary" subsection of the discussion.

	Description	Schematic	Observation supporting (+)/ opposing (—) mechanism	Implications
I	Stable cluster can behave as a nucleus and a condensable species	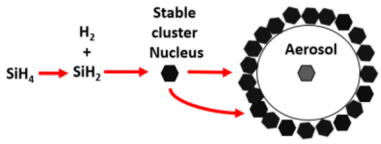	(+) (—) 1, 2,4	The stable cluster can evolve by Brownian collisions following classical aerosol dynamics
II	Stable cluster is a precursor of a nucleus	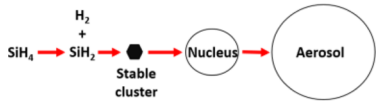	(+) (—) 2,4	The stable polysilicon hydride cannot nucleate on its own, and criteria of the critical cluster cannot be defined solely by a ΔG term.
III	Stable cluster cannot nucleate but can only behave as a condensable species	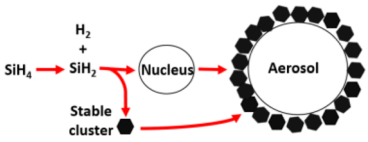	(+) 1, 2, 3, 4 (—)	The stable cluster can condense on pre-existing particles but is not involved in nucleation
IV	Stable cluster plays no role at all in nucleation	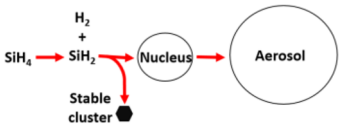	(+)1, 2, 3 (—) 4	The stable cluster is a by-product and does not provide direct information on nucleation or aerosol dynamics

or 10 silicon atoms using real-time aerosol instrumentation, such as the differential mobility analyzers (DMAs). Recent developments of high-resolution differential mobility analyzers (HR-DMAs), however, offer an opportunity to fill the gaps in the measurements. The HR-DMA is able to measure particles below 3 nm with a high sizing resolution and can therefore provide critical physical and chemical information regarding the formation of particles. Many groups have already taken advantages of high flow DMAs to study various systems: the gas phase protein ion density determination,[19] the generation of 1–3.5 nm monomobile particle size standards,[20] the ion composition determination in a corona charger[21] and a radioactive charger,[22] the characterization of functional nanoparticles during combustion,[23,24] and the observation of heterogeneous nucleation.[25]

Like a conventional differential mobility analyzer (DMA), the HR-DMA is composed of two concentric cylindrical electrodes, where an electric field is built across the two electrodes by applying a voltage on the inner electrode. A clean sheath stream flows through the gap of the two electrodes, and at the same time, charged particles are introduced from the inlet slit located at the outer electrode. Due to the balance between the drag force and electrostatic force, under certain inner electrode voltage, only particles with specific sizes are able to be classified and exit through the outlet slit located at the inner electrode, and further measured by using a particle counter (typically an electrometer or a condensation particle counter). More details of the operating principle of the DMA can be found elsewhere.[26,27] Conventional DMAs are not suitable for the measurement of sub-3 nm particles due to the limitation imposed by the high diffusivities of such small particles, which are subject to diffusion losses and inaccuracy caused by the diffusion broadening of the DMA transfer functions.[28] For this reason, the HR-DMA with much higher sheath flow rates, which are above 200 lpm compared to below 20 lpm in conventional DMAs, was developed in recent years, making the measurement of sub-3 nm particles feasible.[29,30] These HR-DMAs have allowed the observation of incipient molecular clusters, providing information on aerosol formation pathways and chemical reaction rates.[23,24,28,31,32] These advantages make the HR-DMA an ideal instrument for the measurement of silicon hydride stable clusters formed during silane pyrolysis.

In this study, the size distributions of stable clusters from silane pyrolysis formed at different conditions were measured using an HR-DMA. Additional characterizations by gas chromatography mass spectrometry (GCMS), transmission electron microscopy (TEM), and gravimetry were conducted to better understand the conditions for the formation of stable clusters. The obtained correlations were compared against expectations from aerosol dynamics. The size of the stable clusters was in agreement with the *ab initio* predictions reported in the literature, but the detection of a comparable signal of clusters at a wide temperature range raises questions on the role of the clusters in nucleation and the initial stages of particle growth. Finally, a discussion on potential mechanistic implications of the cluster in silicon nanoparticle formation is provided. A summary of interesting hypothesized mechanistic routes to be tested in this study is presented in Table I. The column with observations supporting/opposing each mechanism will be debated in the section titled Discussion. Further research is encouraged for assessing the feasibility of the proposed potential mechanistic routes.

The observation number is described in the subsection titled Numbered observation summary.

MATERIALS AND METHODS

The setup used for this study consisted of a silane reactor with a fine control of process parameters and instrumentation. The schematic diagram of the experimental setup is shown in Fig. 1. A 0.9% stream of silane in helium (Airgas, Inc., PA, USA) is controlled using a mass flow controller (MFC) (MKS Instruments, Inc., MA, USA). The second stream is ultrahigh purity helium (99.999% Airgas, Inc., PA, USA), which flows through an oxygen scavenger element (Cee Kay Supply, MO, USA) to eliminate trace amounts of oxygen. The streams were directed into a 1 inch stainless steel 316 tube heated by using a Lindberg furnace (Thermo Fisher Scientific, MA, USA). To minimize the risk of contamination from

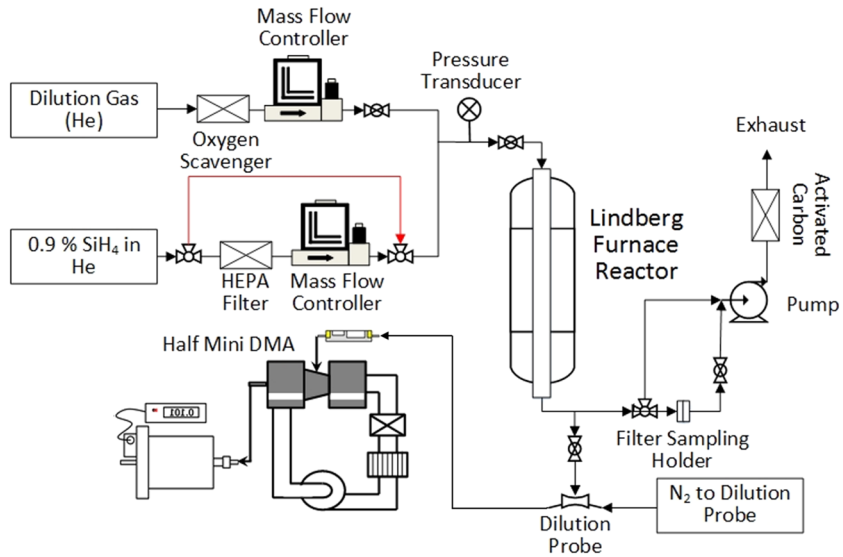

FIG. 1. Experimental silane reactor setup, including ancillary systems and connection to the HR-DMA online mobility diameter characterization instrument.

oxygen and moisture, at the beginning of each run, the whole reactor and feeding lines were purged with a pump until reaching 5 mbar of pressure, then the lines were flushed with a 99.997% nitrogen for about 1 min. The whole purging cycle was repeated 3 times, and the last repressurization was done with 99.999% helium before allowing silane into the reactor. The furnace temperature profile along the center line of the tube was measured using a K type thermocouple (McMaster-Carr, IL, USA). The pressure in the reactor was monitored using a pressure transducer (WIKA, Klingenberg am Main, Germany). Additional details on the reactor can be found elsewhere.[45,46] The sampled stream was diverted from the main flow using a Y with branches at 45°. The primary flow was exhausted through a high capacity filtering medium. The sample was diluted approximately 45 times using a dilution probe composed of a 150 μm flow restrictor orifice in the suction section of a Venturi pump. The dilution gas utilized was nitrogen (99.997% Airgas, Inc., PA, USA). 12.5 lpm of the diluted stream were then introduced into an HR-DMA. Gas chromatography mass spectrometry (GCMS) (Agilent 5975 C Series GC/MSD, Santa Clara, CA, USA) and an RTX 50 gas chromatography column were used to gain insight into the ionic size of the silane clusters. The RTX 50 column consists of a 0.32 mm capillary column packed with methyl polysiloxane. The column was fed by manual injection of gas samples from the reactor outlet using a gas tight 0.5 ml Luer syringe (Restek, Bellefonte, PA, USA), and the column was ramped starting at 30 °C by 10 °C/min to 150 °C and then held for 2 min at 150 °C. Then, the column was baked and flushed up to 300 °C to remove all volatiles from the previous experiment and to condition it for the next measurement. Finally, it was cooled down to 30 °C before starting a new measurement.

An HR-DMA was used to measure the size distribution of sub-3 nm particles generated during silane pyrolysis.[30] The DMA was operated in a closed loop to keep the aerosol inlet and outlet flow equal. The sheath flow of the DMA was provided by using a brushless blower (DOMEL, Inc., Zelezniki, Slovenia), followed by using an inline HEPA filter and a carbon trap to remove the remaining particles in the system. The voltage applied across the DMA electrodes was provided by a high voltage power supply (Bertan 205B, Spellman, Inc., Hauppauge, NY, USA) controlled by using a Labview® program. The voltage was scanned from 0 to 5 kV with a step voltage of 5 V and a step time of 1 s. A homemade Faraday cup electrometer (FCE) was applied downstream from the DMA to count the classified particles. The actual particle concentration was calculated from the electric current monitored by using the FCE and the aerosol flow rate controlled by using the mass flow controller (MKS Instruments, Inc., MA, USA) downstream the FCE. During the experiments, the aerosol flow rate was maintained at 10 lpm. The mobility resolution of the HR-DMA is approximately 10, which was characterized by an earlier study.[28] Hence, the HR-DMA is able to resolve two clusters with a mobility difference of 10%. For a particle smaller than 3 nm, its mobility is inversely proportional to the square of its mobility size. This means that the HR-DMA is able to resolve two clusters with a size difference of around 5%. Three measurements were made at each condition and then averaged to reduce the effect of sample fluctuation. Before experiments, to establish a mobility standard, the high resolution DMA was calibrated by the ions generated from an electrospray of tetraheptyl ammonium bromide (THAB)-methanol solution,[28,33] and the voltages corresponding to the monomer, dimer, and trimer of THAB clusters were recorded. Under the same DMA settings, the product of the mobility of a particle (Z) and the voltage at which the particle is classified (V) remain constant. Hence, the mobility of particles classified at any DMA voltage can be calculated. The mobility size of a particle is further derived by the following equation:

$$Z = Cne/3\pi\mu D_p, \quad (1)$$

where C is the Cunningham slip correction factor, n is the number of charges on the particle, e is the electronic charge, μ is the air viscosity, and D_p is the particle mobility size. For sub-3 nm particles, it is safe to assume that classified particles carry a single charge due to the difficulty in stabilizing more than one charge in such a small volume.[34] Existing studies suggest that the volumetric diameter (D_v) of a sub-3 nm particle is approximately 0.3 nm smaller than D_p due to the influence of the gas molecule's effective diameter.[35] However, the exact relationship is dependent on the material being tested. Further calculation is also needed to derive the exact value of the particle mobility diameter, since the influence of the ion-induced dipole potential on the particle mobility is not evaluated in the Stokes-Millikan equation for sub-3 nm particles.[35,36] For simplicity, the mobility diameter of the particle calculated by Eq. (1) was used to evaluate the particle size distributions in this study. During

TABLE II. Summary of experimental plan and objectives.

No	Test	Technique	Objective	Range	Figure
1	Aerosol collection in the filter	Gravimetry	Observe mass of synthesized aerosols	400–600 °C	2(a)
2	Thermophoretic sampling	TEM	Determine primary particle size distribution and abundance	450–500 °C	2(a)–2(c)
3	Temperature scan of negatively charged clusters	HR-DMA	Observe negatively charged clusters	25–550 °C, 0.6–1.1 nm	3(a)–3(b) and 5(a)
4	Concentration scan negatively charged clusters	HR-DMA	Effect of SiH_4 concentration on cluster behavior	0.019%–0.3% SiH_4	4 and 5(b)
5	Determination of relative concentration of 207 m/z cluster	GCMS	Concentration of 207 m/z cluster	25–550 °C	5(a)

the measurement with the HR-DMA, a Kr-85 radioactive neutralizer (TSI 3077A, TSI, Inc.) was used to charge the particles since silane pyrolysis does not generate charged species.

Aerosols formed at different temperatures were also characterized offline by the following two approaches: The first was to collect the aerosols in a quartz filter for gravimetric analysis. The second was to load aerosols thermophoretically at the outlet of the reactor into a copper grid for TEM analysis. Collection of macroscopic amounts of aerosols was achieved by using 47 mm quartz filters with a thickness of 0.38 mm and no binder. Samples were collected for 5 min and the concentration of SiH_4 used was 0.3%. The filters were located in the interior of a homemade stainless steel filter holder. TEM copper grid sample holders were placed into a thermophoretic sampler located on the outlet of the reactor. The samples were collected for 30 s and then analyzed using a TEM (Fei, Hillsboro, OR, USA). The images were analyzed by converting the TEM images into binary files and analyzed by the pixel count function of ImageJ® 1.48v software.[44] Particle size distributions for conditions above the critical silane concentration were gained by manually counting the primary particles of a representative agglomerate with the aid of ImageJ. To assure representative sampling, more than 40 images were taken in at least 3 different sections of the TEM grid for each sample. All experiments undertaken in this study are summarized in Table II and Table S1 based on the section they are presented.

RESULTS AND DISCUSSION

Critical silane nucleation in the system

The products of silane pyrolysis are capable of inducing new particle formation if its concentration and temperature exceed certain values. At a given temperature, new particle formation occurs only above the critical silane concentration.[37] At concentrations below the critical silane concentration, new particle formation is not observed and no particles are detectable in the gas phase.[38] Similarly, the critical silane temperature indicates the temperature above which new particle formation starts at a given silane concentration. In our reactor, the critical silane temperature for the experiments at 0.3% SiH_4 was not determined accurately. Nevertheless, based on the appearance of observable macroscopic and microscopic aerosol at temperatures higher than 450 °C [Fig. 2(a)], it can be inferred that the critical silane nucleation temperature for our reactor is below such temperature. Figure 2(a) also shows the relative mass gain of the filters, where aerosols were collected for 5 min. The higher the temperature, the more aerosol mass is formed and collected in the filter. The same trend is visible for the increase in aerosol concentration and size at higher temperatures from TEM images. This concentration effect is also visible from the color of the filters, where darker colors are an indication of larger and more abundant aerosols. Due to hydrogen adsorption on the surface of the filters, the weight is displayed as relative weight gain compared to the 400 °C case, where aerosols were neither expected at the given conditions nor visible in the quartz filter. Based on such observations, it is reasonable to expect the critical nucleation temperature for our silane reactor system to lie between 400 °C and 450 °C. This is in contrast with the 490 °C reported by Slootman and Parent.[37] Nevertheless, it is close enough if we consider that the reported critical silane temperatures can differ by more than 100 °C by comparing the results of different authors using analogous systems.[38–40] One explanation of this is that the actual temperature distribution in each system might be substantially different, and the temperature measured by using the thermocouple connected to the furnace display might not reflect the highest temperature in the system (see Fig. S1). Above the critical silane concentration, as the temperature increases, the total aerosol concentration increases as well. This trend was captured by analyzing the projected area from the aerosols compared with the whole area of the TEM image. The results, provided in Fig. 2(b), are consistent with an increase in the total mass concentration of aerosols at higher temperatures. Since the samples were collected thermophoretically, it can be expected that at each temperature, there would be a bias in the amount of the aerosol collected.

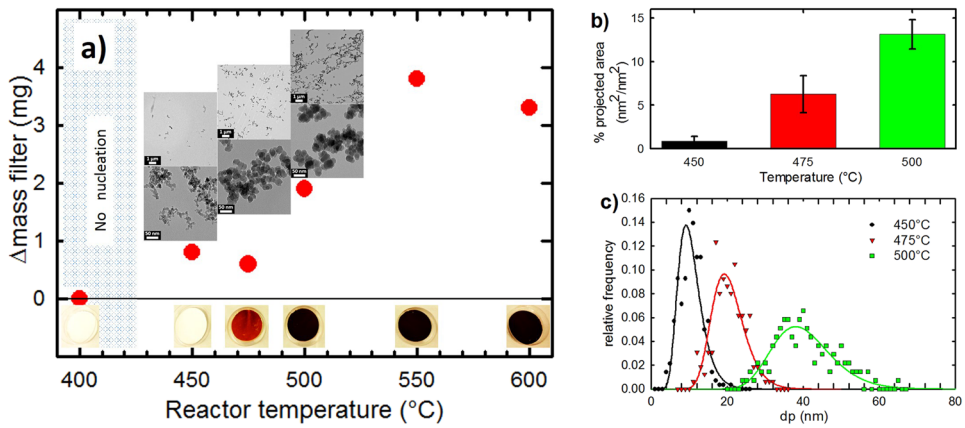

FIG. 2. (a) Mass of aerosols synthesized from 0.3% silane (SiH_4) in He collected in filters for 5 min and TEM images collected thermophoretically for 30 s. Relative mass gain in the filter compared to the 400 °C case. Deviations in the linearity are attributed to filter handling and weighing. (b) Aerosol concentration metrics based on percentage of TEM grid coverage by aerosols. At higher temperatures, higher coverages are seen implying higher aerosol concentration. This information provides the same trend as the filter weight gain from (a) but with more resolution and accuracy (c) The mean size of primary particles also gets larger at higher temperatures.

Nevertheless, such bias is small because the aerosol and gas on the point of thermophoretic sampling are at least 30 cm from the bottom of the reactor. The effect of such bias might cause an additional 1% error in Fig. 2(b), but it would not alter the observed trend significantly. The size distribution of the primary particles within the aerosol agglomerates increases at higher temperatures as well [Fig. 2(c)]. The mean size of the primary particles is 10 nm at 450 °C, 20 nm at 475 °C, and 40 nm at 500 °C, showing a consistent increase in the particle size as the temperature rises.

Neutralizer ions

The measurement of sub-2 nm clusters was achieved with the HR-DMA. This instrument was initially connected directly to the outlet of the reactor but no signal was detectable, which indicates that no ions were naturally present, during the pyrolysis of silane in a helium atmosphere. Such lack of ionic species is common for pyrolysis in furnace aerosol reactors as has been reported in previous studies.[32]

In order to obtain a signal, a neutralizer was mounted between the furnace and the HR-DMA. A neutralizer is a radioactive source of both positive and negative charges that are emitted under steady state. If the aerosols are too small, they cannot stabilize the charge and gas molecular ions are the most stable carriers of the charge. Generally, as aerosols get larger, they are more stable charge carriers, causing ultimately a size-dependent fraction of the aerosols to be charged positive and another fraction negative. Aerosols with both polarities coexist in the aerosol mixture and can be selected and measured based on the voltage polarity set in the HR-DMA. Blanks were measured by using gases at conditions where no aerosol from the furnace was expected. A major and a minor peak at the mobility diameter of 0.67 and 0.90 nm were detected (Fig. S2) and are associated as ion clusters generated from the Kr-85 radioactive neutralizer. Since these peaks are present in many of the measurements in this study, they are referred to as "neutralizer ions" throughout this study. Regular DMAs are not capable of measuring such neutralizer ions, but due to the lower size bounds of the HR-DMA, these gaseous molecular clusters are measurable. The exact chemical identities of the neutralizer ions are not known, but they are likely to be composed of gases used in the dilution train (N_2) and in the reactor (SiH_4 and He) and/or trace gases adsorbed in the neutralizer inner walls. Such molecular ions are attributable to the neutralizer and have also been identified in previous studies.[22,41,42]

Negative cluster ions measured by using the HR-DMA

The size distribution of negatively charged particles generated during silane pyrolysis showed a dynamic response as a function of process parameters. The effect of different temperatures on the size distribution of negatively charged clusters is displayed in Fig. 3. Temperature ranges from 25 °C to 550 °C [Fig. 3(a)] and 420 °C to 490 °C [Fig. 3(b)] at a reactor feed rate of 600 standard cubic centimeters per minute (sccm) and a concentration of 0.3% silane in helium. The size distribution measured at 25 °C [black line in Fig. 3(a)] corresponds to the neutralizer ions. As the furnace temperature increased, this major peak gradually decreased, while new charged species with sizes from 0.65 to 1.0 nm appeared. These intermediate species are produced by the pyrolysis of silane. Unlike the measurements conducted in aerosol reactors with other precursor species, the newly formed species were not composed of molecular clusters with a specific mobility size and did not display the highly resolved peaks observed in those scenarios,[28,31,32] but were rather broad. This suggests that families of molecular ions that might be isomers (share the same chemical formula but with a different molecular structure), or cyclic compounds with different substituents (providing for more or less Si or H atoms in its molecular formula), could have been responsible for the signal and not only an ion with a specific chemical formula and structure. The peak for this signal was reached at 440 °C and quickly diminished when the furnace temperature was increased. The cluster signal completely disappeared at around 550 °C. As shown elsewhere, the temperature for the onset of silicon nucleation and aerosol formation in helium may lie between 450 and 550 °C, and in our measurements, it ranged from 400 to 450 °C. If the signal of the neutralizer ions with peaks at 0.67 nm and at 0.9 nm is removed by deconvolution

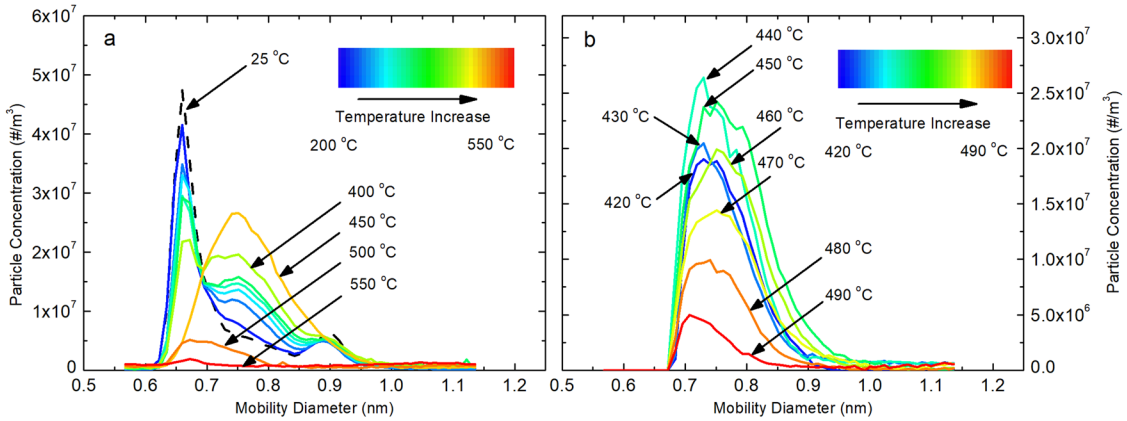

FIG. 3. Negatively charged clusters measured by the DMA in the temperature range of (a) 25 °C–550 °C including the neutralizer ion with a peak around 0.65 nm and (b) 420 °C–490 °C where the neutralizer ions at 0.67 and 0.9 nm have been subtracted using a Gaussian regression.

assuming that they have Gaussian shapes, only the silane clusters remain [Fig. 3(b)].

Positive ions measured by using the HR-DMA

The effect of furnace temperature on the size distribution of positively charged particles was also measured (Fig. S3). However, not a single new peak was observed within the temperatures tested from 25 to 550 °C and HR-DMA detection limits for this experiment (about 0.56–1.14 nm). The only change in the size distribution of positive ions as a function of temperature was a decrease in the signal intensity of the originally detected neutralizer positive ion at higher temperatures, with a more dramatic effect above 500 °C. Such a decrease can be explained by the appearance of larger aerosols that are more stable carriers of the positive charge than the neutralizer ion itself. The scavenging of positive ions by aerosols was less prominent than the one for the negative neutralizer ions at a given temperature. At 550 °C, a remnant peak is visible at the position of the original neutralizer positive ion at 0.78 nm. At the same temperature, the signal from the neutralizer negative peak at 0.7 nm has already disappeared. This indicates that the positive neutralizer ions might have a higher relative affinity for retaining their respective charge in the presence of larger aerosols than their negative counterparts. The absence of species other than neutralizer ions suggests that the intermediate species and nanoparticles generated from silane pyrolysis have a higher affinity for electrons than for positive charges. This electron affinity is also evident when comparing the decrease in negative neutralizer ion species at 500 °C [Fig. 3(a)] vs the decrease in positive neutralizer ions for the same temperature with respect to the room temperature one (Fig. S3).

The effect of silane concentration in silane cluster

Silane concentration also has an effect on the cluster abundance as expected based on mass balance from a simple chemical reaction where the reagent converts into product. This behavior is displayed in Fig. 4 for negative ions. Decreasing silane concentration also lowers the concentration of the produced silicon hydride clusters. Interestingly, this concentration decrease appears to shift the mobility diameter of the silicon hydride clusters toward smaller sizes as well. No effect is observed in the positive ions plot as a function of concentration.

The effect of residence time in silane cluster

Sets of experiments at different residence times were executed to gain a mechanistic understanding of the cluster reaction process at the same temperature (440 °C) and without the influence of concentration (fixed at 0.15%). Results for negative clusters are presented in Fig. S4. The full dynamic range for the reactor MFCs and the flow required by the HR-DMA allowed only a twofold span of residence times. The two fold change provides only 8% difference in the signal of the cluster between the extremes and is too close to the intrinsic instrumental and experimental error to be able to derive any mechanistic conclusion on the effect that residence time has on the silane cluster. However, the relative stability in the signal at different conditions does provide further support to the idea that the cluster, once formed, is rather stable and persistent even at the high

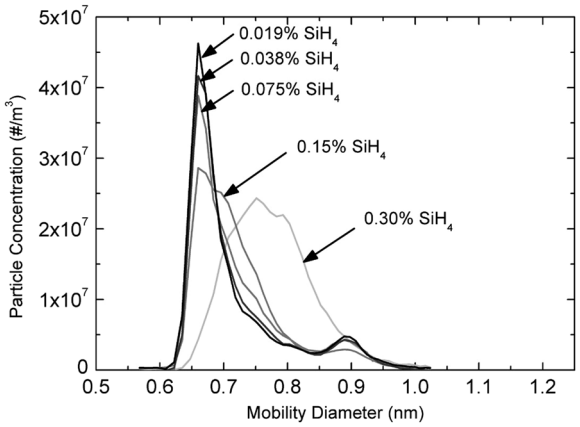

FIG. 4. Negatively charged sub-3 nm particle size distributions measured under different SiH_4 concentrations at 450 °C. The peak at 0.67 nm is generated by the neutralizer, whereas the peak at around 0.75 nm is attributed to the silicon hydride stable cluster. Detection of this cluster below 0.075% SiH_4 was not possible. The peak shifting leftward instead of downward (compare to Fig. 3) suggests that the formation of this cluster is enhanced at higher concentrations of silane and lower concentrations of the last might produce smaller clusters.

temperatures in the reactor. Similarly, no significant effect was observed for positive ions.

Gas chromatography mass spectrometry

Gas chromatography mass spectrometry (GCMS) was used to gain information on the chemical composition of the stable silicon cluster. The GCMS m/z spectral results of the reactor blank (without silane) and with 0.3% silane in helium at 450 °C are compared in Fig. S5a. In Fig. S5b, the selected chromatograms for Si, SiH_4, and potential silicon hydride clusters (Si_nH_m) are compared for the 450 °C and the blank condition. For the case with silane at 450 °C, a peak not present in the blank at 207 and another at 281 m/z were observed. These m/z are consistent with an Si_7H_{11} and $Si_{10}H_1$ ion, which are likely produced when ionizing a stable silicon hydride polymer, but these might also be fragments of larger stable clusters that lose some of their mass when ionized before the MS. Figures S5c and S5d show the chromatograms of the ion 207 and 281 m/z at different temperatures. The chromatogram for ion 207 shows broad peaks between 1–3 min and 5.5–6.5 min. For the case of ion 281, the broad peak appears at 8.5 min. A reasonable approach to interpret the chromatograms for 207 m/z is to assume that the first peak is related to both gases that do not interact with the column and aerosols that are pushed through the column by the carrier gas. This is also supported by the large peak for Si and SiH_4 in this time domain. The peak at 6 min is considered to be due to the clusters in the gas phase; the fact that at 400 °C no aerosols are expected and the first peak is not observed in Fig. S5c supports this interpretation. Finally, the signal in between the 2 peaks at time from 2.5 to 5.5 min could be attributed to insufficient chromatographic separation, to the presence of several isomers with the same molecular weight, to the condensable species being released at different points inside the chromatographic column as the silicon nanoparticles collide and bounce, or to a combination of these factors. Since these

compounds were virtually the only ones with m/z > 100 detectable by GCMS, and their size is comparable with the one of the silicon hydride cluster signals obtained via the HR-DMA, it is plausible that both measurements refer to the same molecules.

Aerosols are expected to move with linear velocities of around 0.2 m/s but might occasionally collide with the capillary walls. Such collisions should not be strong enough to break the components of the particle that are chemically bonded with the solid nanoparticle scaffold. Nevertheless, the clusters that can be measured at 207 m/z might not be chemically bonded to the nanoparticle but rather just adhered with a mechanism that is weaker, such as van der Waals forces and, which upon contacting the packing material, might adhere to it more effectively and get removed from its original aerosol carrier. This would explain the noisy appearance of the cluster signal at conditions where aerosols are present (above 400 °C), but not at conditions where no aerosols are formed. This is explained by the fact that the aerosols move much faster than the clusters and interact less with the column due to a higher mass to surface ratio. Nevertheless, these aerosols might release such a cluster through the whole column as the aerosols travel through and get exhausted within the first 2.5 min of the GCMS measurement. This is supported by the silicon signal that is over at 2.5 min in the chromatogram (Fig. S5b).

Based on a simple calculation that takes into consideration the covalent radius of silicon atoms, the size range that the ions with m/z = 207 and 281 can have is between 0.45 nm and 1.2 nm depending on the actual chemical structure of the cluster, where the smallest value is obtained considering a closed octahedral shape and the second a perfectly linear shape. This suggests that the ions measured by GCMS could be the same ions as those measured by using the HR-DMA and could also correspond to the critical clusters identities reported in the literature to contain 7 or more silicon atoms.[16]

DISCUSSION

In order to better understand the experimental results, it is important to clarify that in addition to only measuring within its size range, an HR-DMA requires the following in order to be able to measure clusters. If any of these points is not met, the clusters cannot be detected.

(1) The measured cluster ion and/or its precursor should be stable enough as to pass through the reactor, then through the dilution probe, the neutralizer, and finally inside the HR-DMA.
(2) The molecular ion cluster needs to be capable of acquiring and retaining a positive or negative charge between the neutralizer and the FCE detector.
(3) Enough clusters need to be present and they should be stable enough compared to the rest of the mix of aerosols/molecules in the carrier gas so that a number of clusters higher than the detection limits of the HR-DMA can be achieved.

Point 1 is met for the reported cluster at the wide range of temperatures tested and with the sampling system utilized. Point 2 is met by the cluster for the negative polarity but is not met for the positive polarity. Therefore, no positively charged clusters are observed (Fig. S3). Point 3 is a limitation to measure conditions at lower concentrations than 0.1% SiH_4 in our system (Fig. 4).

Temperature dependence of the observed intensity of the cluster signal

The presence of the discussed high molecular weight silicon hydride with a mobility diameter peak at 0.75 nm can be detected by the HR-DMA at temperatures as low as ~200 °C (Fig. 3), and at ~440 °C it reaches a maximum. Above this temperature, by following Arrhenius kinetic behavior, it would be expected that the concentration of stable silicon hydrides produced may be even larger, following an exponential growth. However, their measured concentration at the outlet of the reactor decreased [Fig. 5(a)]. Interestingly, the concentration measured based on GCMS shows a fairly constant concentration of the 207 m/z ion after 450 °C. Based on the ΔG criteria for the formation of stable clusters, it would be expected that, as with the critical silane concentration, silicon hydride stable clusters

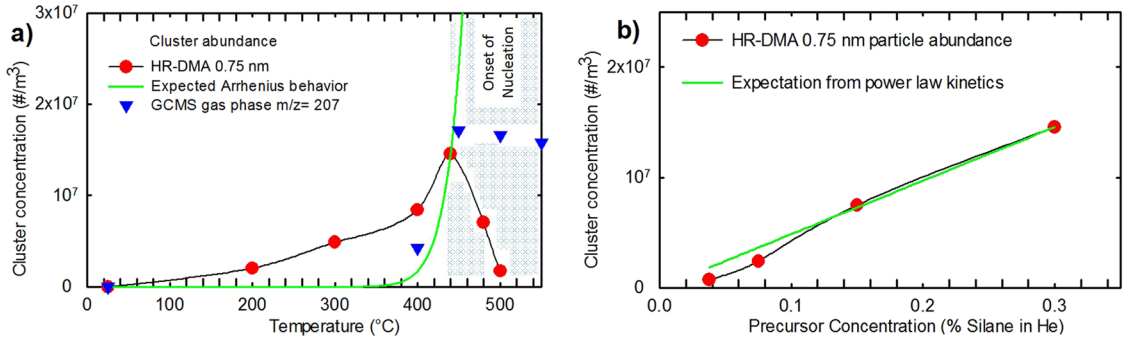

FIG. 5. (a) Expected behavior based on Arrhenius temperature dependence. The data were obtained from 0.3% SiH_4 runs at various temperatures. If the cluster formation were limited by the kinetics of polymerization of silicon hydrides, with limiting step based on the formation of silylene, it should show an Arrhenius behavior. The fact that it does not follow it is surprising and suggests the cluster is formed by a different mechanism. The GCMS gas phase m/z = 207 corresponds to the clusters measured at such a molecular weight for the 5.5–6.5 min in the chromatogram for the given temperatures. (b) The formation of the cluster at 450 °C follows the expectation from power law kinetics as a direct function of precursor concentration and is an indication that the signal obtained from the HR-DMA is proportional to the expected concentration of the cluster.

might be composed of polymers of different sizes at different temperatures and concentrations. In the numerous polymerization processes that occur in silane pyrolysis, the equilibrium and kinetic constants are modified as the synthesis temperature is changed. Thus, based on such argument, the point at which a reaction becomes predominantly irreversible may change and clusters of different sizes could become more predominant. However, the size distribution of the measured cluster does not seem to shift significantly and therefore appears to be made of the same cluster constituents for synthesis temperatures between 200 and 550 °C. This does not disprove the formation of higher molecular weight stable clusters but indicates that even if they form, they are not detectable with the instruments used in this study.

Translating HR-DMA signal into a silicon hydride concentration: Applicability and limitations

Care should be taken when converting the signal measured by using the HR-DMA into a concentration. This is important to consider to ensure that the maximum at 440 °C in Fig. 5 is not a consequence of such an effect. Attributing causality to the decrease in concentration of the cluster is not straight forward because competing, consecutive, and parallel processes might occur simultaneously. Two important comments follow:

(1) The larger particles formed above ~450 °C can be consuming the silicon hydride clusters through condensation, either physically or chemically, due to the ever increasing surface area available of aerosols forming at increasing rates as temperatures rise.[43]
(2) Charging efficiency is sometimes considered to be solely a function of particle size, but the presence of more stable charge carriers also plays a role. In the same way that the neutralizer ion disappears when the silicon hydride stable cluster appears as the last might be a more stable charge carrier. Although this may be confirmed by calculating the ion flux on the particles generated under different temperatures, one needs to know the actual number of particles in the neutralizer, which is very challenging due to the unknown charging efficiency. The silicon hydride stable cluster signal might also disappear because a more stable charge carrier appears in the system (aerosols of several nanometer), above ~450 °C, but that are beyond the detection limits of the HR-DMA. This interpretation is consistent with the fairly constant concentration of the 207 m/z species in the gas phase (retention time between 5.5 and 6.5 min) above 450 °C measured by GCMS (Fig. 5). Furthermore, the presence of a larger amount of aerosols explains the neutralizer ions being progressively depleted as the temperature rises because more aerosols are available to scavenge the ion charges for both negative [Fig. 3(a)] and positive ions (Fig. S3), in agreement with previous studies.[28]

The effect of concentration tested at 450 °C summarized in Fig. 5(b) shows that at least for this condition, the HR-DMA signal for the cluster is proportional to the precursor concentration, as expected for a power law reaction kinetics. This is an indication that in this regime, the HR-DMA does provide a signal proportional to the gas phase concentration of the cluster in the reactor. A similar behavior can be inferred for temperatures lower than the critical silane temperature where no aerosols form.

Lack of Arrhenius correlation of the cluster

In order to extract mechanistic insight into the dependence of the silicon hydride clusters, the dependence of cluster concentration was observed as a function of temperature [Fig. 5(a)] and concentration [Fig. 5(b)] while keeping all other variables constant. The results were compared with standard Arrhenius dependences and power law kinetics. It was found that the cluster concentration does not follow an exponential temperature dependence as Arrhenius type of kinetics would predict. Interestingly, the cluster concentration increases as a function of silane concentration in agreement with a process following power law kinetics. This is consistent with the measurement of the silane cluster representing the actual concentration of the cluster in the gas phase at 450 °C.

The fact that the cluster is not following Arrhenius dependence as a function of temperature from 25 to 450 °C suggests that there could be a complex reaction mechanism where the rate limiting step is not dominated by the activation energy of a collision event such as silylene formation. The decrease in the cluster concentration above 450 °C on the other hand can be explained by the appearance of aerosols that scavenge the cluster.

Possible mechanistic roles of the stable cluster in new particle formation

It is challenging, yet important to try to understand the mechanistic role that the observed stable cluster might be playing in new particle formation. A summary of potential roles that the silicon stable cluster is playing in the initial stages of aerosol dynamics was introduced in Table I. In section titled Numbered observation summary, important observations of all experimental sections are analyzed to determine the feasibility of the potential mechanisms. The experimental observations are numbered and summarized as follows.

Numbered observation summary

(1) Presence of stable cluster already at 200 °C (~250 °C below critical silane temperature for 0.3% SiH_4).
(2) Size distribution never shifting rightward up to 1.2 nm, where clusters of silicon hydride dimers and trimers would lay within instrumental detection limits. Either they do not form or they are incapable of remaining stable upon being charged.
(3) Decrease in HR-DMA signal above 450 °C might be a charge depletion effect.
(4) GCMS appearance of additional peak above 450 °C at 1–3 min and noise between this and the peak at 5.5–6.5 min.
(5) Lack of Arrhenius behavior for the formation of silicon hydride clusters between 25 and 450 °C.

Mechanism I: Cluster can behave as a nucleus and also as a condensable species

This is the mechanism that would obey classical aerosol dynamics. Silane reacts upon forming a molecule that is stable and crosses

the dΔG/dn = 0 barrier, evolving further by aerosol dynamics based on Brownian collisions and being capable of both behaving as a stable nucleus and also causing condensation. Evidence against this interpretation includes the fact that the stable cluster is observed already at 200 °C, but no evidence of larger aerosols is seen until ~450 °C. No observation in this study supports directly this mechanism.

Mechanism II: Stable cluster is a precursor of a nucleus

This explanation is reasonable from a mechanistic point of view since it considers the polysilicon hydride as a step in nucleation, yet not the critical one for phase change. Observations against this mechanism include the absence of measurable aerosols larger than the cluster and within the detection range of the HR-DMA and the fact that GCMS data do not provide support for this mechanism. The cluster being present at 200 °C but nucleation occurring until ~450 °C is not completely antagonistic against this mechanism, but it makes it less likely.

Mechanism III: Stable cluster is not a nucleus but behaves as a condensable species

Based on the observable properties of the silicon hydride cluster measured using high resolution DMA, several facts are consistent with an interpretation where the cluster is behaving as a condensable species rather than as a critical silicon nucleus: The observations that are consistent with this interpretation are the following: the size distribution of the cluster as shown in Fig. 3 is broad (0.65–0.95 nm), yet it appears static (cluster not interacting with monomers) and not growing in terms of mobility as would be expected for a nucleus after receiving surface growth or condensation from monomers. It seems unlikely that if the cluster was a critical nucleus, a larger, continuous size distribution would never appear despite scanning through broad ranges of temperatures (200–550 °C), as well as at various precursor concentrations and residence times, spanning a wide range of reaction rates. Furthermore, when comparing the cluster concentration displayed in Fig. 3 with the TEM images of aerosols presented in Fig. 2, it becomes evident that a whole range of condensable species is available for causing the cluster to grow from very few as in the 450 °C or lower temperatures and up to a significant amount of condensable species in the 500 °C case. However, in neither case is the cluster size distribution in Fig. 3(a) a continuous distribution that goes beyond 1 nm. Furthermore, silicon nucleation from silane pyrolysis has been reported to be an abrupt phenomenon that occurs at the critical silane temperatures for a given concentration (~450 °C for 0.3% SiH_4). However, Fig. 3 shows that the appearance of the cluster is gradual starting at least around 200 °C, much below the conditions where aerosols start to be detected both by the presented experimental results of this work in Fig. 2, as well as by the reported value in the literature,[37] which is around 450 or 500 °C for the 0.3% SiH_4 concentration in helium. All of these facts support the interpretation of this cluster behaving as a condensable species and not as a silicon critical nucleus. The implications of such interpretation suggest that there could be important additional parameters to the criteria of dΔG/dn = 0 for defining the moment when a cluster becomes a critical nucleus and the criteria necessary for defining a critical nucleus in chemical reaction systems should be further studied.

Mechanism IV: Stable cluster playing no role at all in nucleation

Another interpretation is to look at the cluster as a molecular ion without any role in aerosol formation and growth. Such an interpretation is disappointing from the aerosol dynamics perspective and would imply that the cluster behaves neither as a nucleus nor as a condensable species. This interpretation, however, would be useful in terms of knowing that it is necessary to search for another molecule/cluster in nucleation. Nevertheless, the GCMS signal opposes this mechanism because of the signal of the cluster being present in the noisy region between the cluster in the aerosols peak and the cluster in the gas phase peak.

CONCLUSIONS

Stable high molecular weight clusters formed during silane pyrolysis were measured for the first time using a high-resolution DMA. The determined mobility size peaks around 0.75 nm. GCMS shows a peak at 207 m/z and a smaller one at 281, which is compatible with a tentative molecular ionic identity of Si_7H_{11} and $Si_{10}H_1$, respectively. TEM images provide information on the abundance of aerosols as well as their primary particle size distribution at different conditions. The experimental results were analyzed as a function of process parameters to provide insights into the silicon hydride stable cluster behavior. The observations were then used to compare the feasibility of four interesting potential mechanistic roles the cluster could be playing in nucleation.

GCMS provided m/z measurements of the fragments of stable clusters. However, it is not clear what the original cluster size was. The progressive formation of aerosols as temperature rises beyond the onset of critical silane concentration is evidenced by silicon nanoparticle TEM images as well as from filter collection and neutralizer-generated ions, both positive and negative, becoming scarce after 500 °C. The high molecular weight silicon hydride cluster is measurable above ~200 °C for 0.3% SiH_4 in He. It peaks at 440 °C and disappears gradually at higher temperatures. The fading of the peak can be explained by the appearance of more available aerosols that either physically scavenge the silicon hydride clusters or are more stable carriers of the neutralizer charges, thus lowering the amount of the measurable silicon hydride cluster by using an HR-DMA.

The rate limiting mechanism for silicon hydride cluster formation is consistent with a process that is a function of silane concentration. However, the cluster does not follow the expected Arrhenius behavior of power law kinetics as a function of temperature. This is in contrast to the first order reaction kinetics suggested in the literature as the limiting step for the overall formation of silicon from silane pyrolysis. This suggests that the rate limiting step for the formation of this cluster might not be governed by a (classical) collision/thermal activation process and is not a strong function of temperature as expected for an Arrhenius behavior.

Different mechanisms were analyzed, and the observations of this study were categorized as supporting or opposing such mechanisms. Further research is necessary to fully validate a given

mechanism. If proven valid, the mechanistic implications in each case have been outlined and could provide interesting consequences for our understanding of the role of stable clusters in new particle formation and growth. The mechanism with more evidence supporting it is the one that sees the cluster as a condensable species only, incapable of behaving as a critical nucleus. One important consequence of this mechanism (III) is that it calls for the need to find alternative/additional parameters to determine at what point a cluster will behave as a critical nucleus, which, up to now, has sometimes been assumed to be determined by the $d\Delta G/dn = 0$ of cluster formation.

The data presented in this study are on their own not sufficient to settle a particular interpretation on the role of subnanometer clusters in nucleation. On the contrary, the evidence presented is on its own valuable as it is used to raise awareness that there are important questions to be addressed on the classical assumptions of nucleation and aerosol dynamics starting from chemical reactions. Some classical assumptions seem less likely than alternative explanations here suggested, but they require further research to increase the certainty of their mechanistic interpretations.

SUPPLEMENTARY MATERIAL

See the supplementary material for the temperature distribution of the furnace, high resolution DMA blank, positive ion and residence time measurements, as well as a summary of the GCMS spectra corresponding to different temperatures.

ACKNOWLEDGMENTS

We would like to thank Danny Sales and Martin Yamane for their help in temperature profile data acquisition and other reactor characterizations useful for this study. This work was partially supported by the Solar Energy Research Institute for India and the United States (SERIIUS), funded jointly by the U.S. Department of Energy (Office of Science, Office of Basic Energy Sciences, and Energy Efficiency and Renewable Energy, Solar Energy Technology Program, under Subcontract No. DE-AC36-08GO28308 to the National Renewable Energy Laboratory, Golden, Colorado) and the Government of India through the Department of Science and Technology under Subcontract No. IUSSTF/JCERDC-SERIIUS/2012. The Nano Research Facility (NRF) at Washington University in St. Louis, a member of the National Nanotechnology Infrastructure Network (NNIN), was used for TEM.

REFERENCES

[1] B. Caussat, M. Hemati, and J. P. Couderc, Chem. Eng. Sci. **50**, 3615 (1995).
[2] B. Caussat, M. Hemati, and J. P. Couderc, Chem. Eng. Sci. **50**, 3625 (1995).
[3] W. Filtvedt *et al.*, Sol. Energy Mater. Sol. Cells **94**, 1980 (2010).
[4] M. Zbib *et al.*, J. Mater. Sci. **45**, 1560 (2010).
[5] J. R. Szczech and S. Jin, Energy Environ. Sci. **4**, 56 (2011).
[6] X. Zhou *et al.*, Chem. Commun. **48**, 2198 (2012).
[7] J. G. Martin, H. E. Oneal, and M. A. Ring, Int. J. Chem. Kinet. **22**, 613 (1990).
[8] K. Yoshida *et al.*, J. Phys. Chem. A **110**, 4726 (2006).
[9] A. A. Onischuk *et al.*, J. Aerosol Sci. **28**, 207 (1997).
[10] M. A. Ring and H. E. O'Neal, J. Phys. Chem. **96**, 10848 (1992).
[11] S. L. Girshick *et al.*, J. Electrochem. Soc. **147**, 2303 (2000).
[12] D. M. Kremer *et al.*, J. Cryst. Growth **247**, 333 (2003).
[13] C. J. Giunta *et al.*, J. Appl. Phys. **67**, 1062 (1990).
[14] C. Kleijn, J. Electrochem. Soc. **138**, 2190 (1991).
[15] M. T. Swihart and S. L. Girshick, Chem. Phys. Lett. **307**, 527 (1999).
[16] H. W. Wong *et al.*, J. Phys. Chem. A **108**, 10122 (2004).
[17] M. T. Swihart and S. L. Girshick, J. Phys. Chem. B **103**, 64 (1999).
[18] S. Nijhawan *et al.*, J. Aerosol Sci. **34**, 691 (2003).
[19] A. Maißer *et al.*, Phys. Chem. Chem. Phys. **13**, 21630 (2011).
[20] M. Attoui *et al.*, Aerosol Sci. Technol. **47**, 499 (2013).
[21] H. Manninen *et al.*, Atmos. Meas. Tech. **4**, 2767 (2011).
[22] G. Steiner *et al.*, Aerosol Sci. Technol. **48**, 261 (2014).
[23] Y. Wang *et al.*, Combust. Flame **176**, 72 (2017).
[24] Y. Wang *et al.*, Proc. Combust. Inst. **36**, 745 (2017).
[25] P. M. Winkler *et al.*, Science **319**, 1374 (2008).
[26] M. R. Stolzenburg and P. H. McMurry, Aerosol Sci. Technol. **42**, 421 (2008).
[27] E. Knutson and K. Whitby, J. Aerosol Sci. **6**, 443 (1975).
[28] Y. Wang *et al.*, J. Aerosol Sci. **71**, 52 (2014).
[29] J. Fernandez de la Mora, *Aerosol Measurement: Principles, Techniques, and Applications*, 3rd ed. (John Wiley & Sons, 2011), p. 697.
[30] J. F. de la Mora and J. Kozlowski, J. Aerosol Sci. **57**, 45 (2013).
[31] J. Fang *et al.*, Anal. Chem. **86**, 7523 (2014).
[32] Y. Wang *et al.*, J. Nanopart. Res. **17**, 1 (2015).
[33] S. Ude, J. Fernandez de la Mora, and B. Thomson, J. Am. Chem. Soc. **126**, 12184 (2004).
[34] W. Hoppel and G. Frick, NRL Report No. 9108, DTIC Document, 1988.
[35] C. Larriba *et al.*, Aerosol Sci. Technol. **45**, 453 (2011).
[36] B. K. Ku and J. F. de la Mora, Aerosol Sci. Technol. **43**, 241 (2009).
[37] F. Slootman and J.-C. Parent, J. Aerosol Sci. **25**, 15 (1994).
[38] F. Eversteijn, Philips Res. Repts **26**, 134 (1971).
[39] S. Iya, R. Flagella, and F. DiPaolo, J. Electrochem. Soc. **129**, 1531 (1982).
[40] T. Murthy *et al.*, J. Cryst. Growth **33**, 1 (1976).
[41] A. Maißer *et al.*, J. Aerosol Sci. **90**, 36 (2015).
[42] G. Steiner and G. P. Reischl, J. Aerosol Sci. **54**, 21 (2012).
[43] S. S. Talukdar and M. T. Swihart, J. Aerosol Sci. **35**, 889 (2004).
[44] W. S. Rasband, ImageJ, U.S. National Institutes of Health, Bethesda, Maryland, USA, http://imagej.nih.gov/ij/, 1997–2015.
[45] M. Vazquez-Pufleau and M. Yamane, Chem. Eng. Sci. **211**, 115230 (2019).
[46] M. Vazquez-Pufleau, "The effect of nanoparticle morphology in the filtration efficiency and saturation of a silicon beads fluidized bed," AIChE J. (published online).